© 2016. Published by The Company of Biologists Ltd | Development (2016) 143, 1823-1831 doi:10.1242/dev.132753

TECHNIQUES AND RESOURCES

RESEARCH ARTICLE

Sebaceous lipids are essential for water repulsion, protection against UVB-induced apoptosis and ocular integrity in mice

Maik Dahlhoff[1], Emanuela Camera[2], Matthias Schäfer[3], Daniela Emrich[4], Dieter Riethmacher[5,6], April Foster[7], Ralf Paus[7] and Marlon R. Schneider[1,*]

ABSTRACT

Sebocytes, which are characterized by lipid accumulation that leads to cell disruption, can be found in hair follicle-associated sebaceous glands (SGs) or in free SGs such as the Meibomian glands in the eyelids. Because genetic tools that allow targeting of sebocytes while maintaining intact epidermal lipids are lacking, the relevance of sebaceous lipids in health and disease remains poorly understood. Using *Scd3*, which is expressed exclusively in mature sebocytes, we established a mouse line with sebocyte-specific expression of Cre recombinase. Both RT-PCR analysis and crossing into *Rosa26-lacZ* reporter mice and $Kras^{G12D}$ mice confirmed Cre activity specifically in SGs, with no activity in other skin compartments. Importantly, loss of SCD3 function did not cause detectable phenotypical alterations, endorsing the usefulness of *Scd3-Cre* mice for further functional studies. *Scd3-Cre*-induced, diphtheria chain A toxin-mediated depletion of sebaceous lipids resulted in impaired water repulsion and thermoregulation, increased rates of UVB-induced epidermal apoptosis and caused a severe pathology of the ocular surface resembling Meibomian gland dysfunction. This novel mouse line will be useful for further investigating the roles of sebaceous lipids in skin and eye integrity.

KEY WORDS: Sebaceous glands, Mouse, Gene targeting, Water repulsion, Meibomian gland disease

INTRODUCTION

The term 'sebocyte' describes a type of epithelial cell that differentiates by progressive cytoplasmic lipid accumulation, leading to breakdown and discharge of the entire cell, a unique type of exocrine secretory mechanism called holocrine secretion (Schneider and Paus, 2010; Thody and Shuster, 1989). The prototype sebocyte is found in hair follicle-associated sebaceous glands (SGs), that produce sebum consisting essentially of triglycerides, wax esters, squalene (in humans only) and free fatty acids (Smith and Thiboutot, 2008). Sebum is reported to be important for skin and hair coat waterproofing, and its antioxidative and antimicrobial properties have led to the assumption that it is also important to maintain the epidermal barrier (Hinde et al., 2013; Schneider and Paus, 2010; Tóth et al., 2011). In addition to the hair follicle, sebocytes are found at several other locations of the mammalian body, forming so-called free or ectopic SGs, which are anatomically restricted and enlarged or otherwise modified. A well-known example of ectopic SGs are the Meibomian glands, which are located in both the upper and lower eyelids. The complex mixture of lipids (meibum) synthesized by the sebocytes (meibocytes) in these glands is delivered to the outer surface of the eye, where it forms the tear film lipid layer, which is essential for maintaining the ocular surface health and integrity (Knop et al., 2011). Rodent preputial glands, which produce pheromones important for territorial marking, also contain a high proportion of sebocytes. Other locations include: the nipple of the female breast, the genitals and the ear canal. Importantly, sebocyte dysfunction is associated with a number of diseases. Increased sebum release and changes in sebum composition are a key component in the pathogenesis of acne, the most common skin disease of adolescence (Williams et al., 2012). Meibomian gland dysfunction, which is characterized by terminal duct obstruction and/or qualitative/quantitative changes in meibum composition, is the leading cause of dry eye disease (Nelson et al., 2011).

Research on sebocyte-associated pathophysiology has been hampered by two major obstacles. First, accurate *in vitro* models recapitulating full sebaceous differentiation culminating in holocrine secretion are lacking. Second, sebocyte gene-targeting studies *in vivo* have so far used regulatory sequences of keratin genes or other structural proteins (Schneider, 2012). Although effective, this strategy has the disadvantage that numerous cell types in the epidermis and in the pilosebaceous unit are targeted in parallel, potentially causing side effects and unspecific phenotypes. Skin-specific ablation of genes such as *Scd1* (Sampath et al., 2009) or *Acbp* (Neess et al., 2013) using the keratin 14 (*Krt14*) promoter revealed a role of cutaneous lipogenic pathways in whole-body energy balance; however, this strategy does not permit differentiation between the role played by epidermal versus sebaceous lipids.

In the present study, we employed the *Scd3* gene, which encodes an enzyme expressed in sebocytes only (Zheng et al., 2001), to establish a mouse line with sebocyte-specific expression of Cre recombinase. After detailed characterization of this novel mouse line, we investigated the functions of sebaceous lipids using a toxin-based cell lineage ablation approach.

RESULTS

Scd3-Cre mice show sebocyte-specific expression of Cre

To create a mouse line with sebocyte-specific expression of Cre recombinase, we replaced the first exon of *Scd3*, a gene encoding an enzyme of the stearoyl-coenzyme A desaturase family that is expressed exclusively in differentiated sebocytes (Zheng et al., 2001) with the cDNA for codon-improved Cre recombinase via

[1]Institute of Molecular Animal Breeding and Biotechnology, Gene Center, LMU Munich, Munich 81377, Germany. [2]Laboratory of Cutaneous Physiopathology and Integrated Center of Metabolomics Research, San Gallicano Dermatologic Institute, IRCCS, Rome 00144, Italy. [3]Institute of Molecular Health Sciences, ETH Zurich, 8093 Zurich, Switzerland. [4]Institute of Veterinary Pathology, Center for Clinical Veterinary Medicine, LMU Munich, Munich 80539, Germany. [5]School of Medicine, Nazarbayev University, Astana 010000, Kazakhstan. [6]Human Development and Health, Faculty of Medicine, University of Southampton, Southampton SO16 6YD, UK. [7]Centre for Dermatology Research, Institute of Inflammation and Repair, University of Manchester, Manchester M13 9PT, UK.

*Author for correspondence (marlon.schneider@lmu.de)

Received 6 November 2015; Accepted 9 March 2016

Development (2016) 143, 1823-1831 doi:10.1242/dev.132753

homologous recombination in embryonic stem cells (Fig. 1A). After identification of cells carrying the desired mutation (clone A10, Fig. 1B), we generated germline chimeras by blastocyst injection. RT-PCR analysis confirmed that expression of *Scd3* and *Cre* was limited to back and tail skin and to the Harderian and preputial glands of *Scd3-Cre* animals (Fig. S1A). Importantly, no expression of *Scd3* or *Cre* was detected in brown adipose tissue or in four different white adipose tissue depots of *Scd3-Cre* animals (Fig. S1A). The positive offspring was crossed to the *Rosa26-lacZ* reporter line to functionally assess Cre-mediated recombination of the reporter locus using histochemical detection of β-galactosidase (β-gal). Cre activity, reflected by blue staining, was detectable in double heterozygous animals at postnatal day (P) 4, when groups of lipid-filled sebocytes appear for the first time in mouse back and tail skin (Fig. 1C). No Cre activity was detectable in embryonic skin or in the skin of newborn mice [embryonic day (E) 17.5 and P0, respectively; data not shown]. A clear and robust blue staining was also observed in the SGs of adult double heterozygous mice. Importantly, at all time points Cre activity was restricted to the SGs, with no staining in the epidermis, dermis or hair follicle in both back and tail skin (Fig. 1C). Immunofluorescence staining for β-gal (which reflects Cre expression) and E-cadherin (which marks all epithelial cells of the SG) showed that β-gal expression is robust in differentiated sebocytes in the middle of the SG, but almost undetectable in the undifferentiated sebocytes that line the gland (Fig. 1D). This finding confirms previous data on *Scd3* expression obtained by other authors using *in situ* hybridization (Zheng et al., 2001).

In adult double heterozygous mice, Cre expression was also clearly visible in the Meibomian and preputial glands, which are both well-known sebocyte-bearing structures (Fig. S1C). However, although Cre-induced recombination was robust and extensive in Meibomian glands, *Scd3-Cre* activity affected only a small proportion of sebocytes in preputial gland (Fig. S1C). We also detected a small number of β-gal^{+} cells in the intestinal epithelium and in the cerebral cortex (Fig. S1C). In summary, *Scd3-Cre* mice represent a powerful tool for specifically targeting sebocytes without affecting other epidermal cells.

Absence of *Scd3* expression in *Scd3-Cre* homozygous mice has no overt phenotypical consequences

RT-PCR analysis was used to assess whether the targeted *Scd3-Cre* allele represents a *Scd3* knockout allele. While *Scd3* transcripts were readily detectable in the preputial gland and the skin of heterozygous *Scd3-Cre* mice, no *Scd3* expression was detected in homozygous animals (Fig. S2A). Loss of SCD3 protein was confirmed using immunofluorescence (Fig. S2B). *Scd3-Cre*$^{+/+}$ mice grew normally, were fertile, and showed no gross phenotype

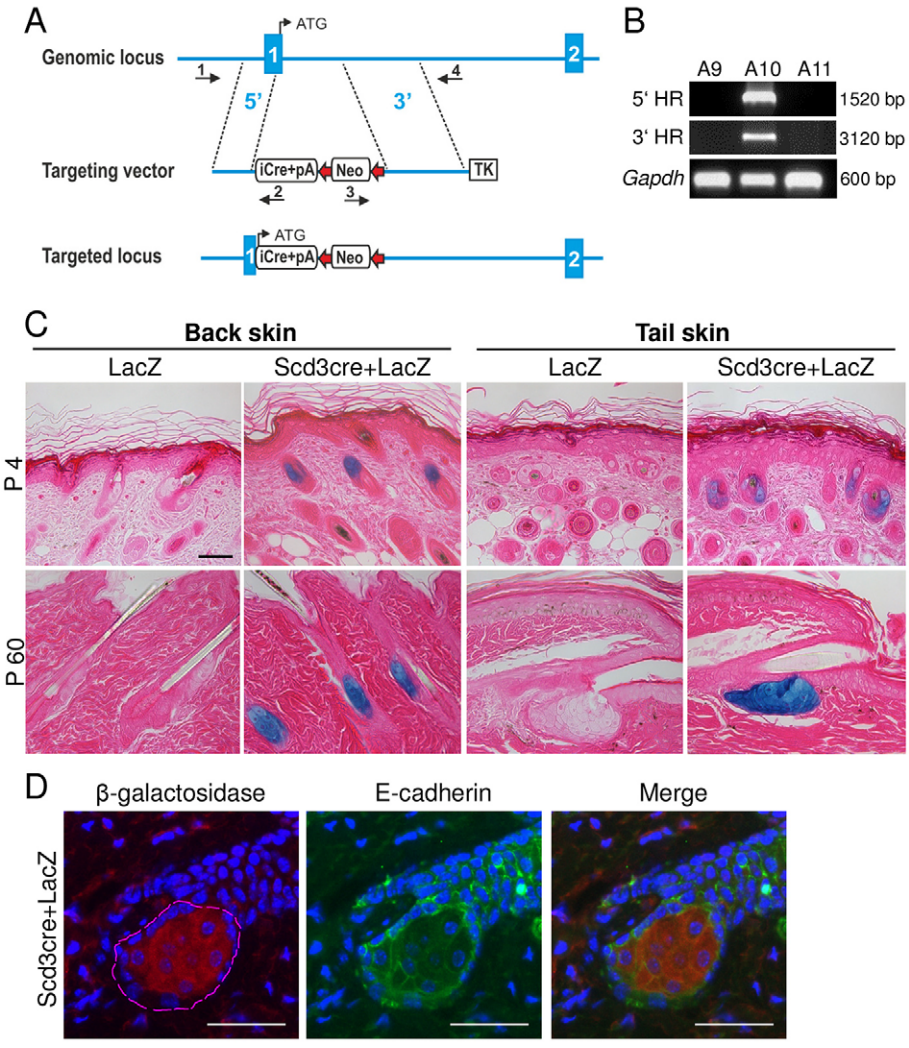

Fig. 1. Generation of *Scd3-Cre* mice. (A) The targeting vector, including 5′ and 3′ homology arms, the iCre sequence, a FRT-flanked neomycin cassette and a TK cassette for negative selection, was designed to replace exon one of *Scd3* (containing the first ATG) with the *Cre* cDNA. (B) Confirmation of homologous recombination at 5′ and 3′ ends in clone A10 by PCR. (C) Crossing *Scd3-Cre* mice into the reporter line *Rosa26-lacZ* and staining for β-galactosidase activity revealed that Cre activity is restricted to the sebaceous gland in both newborn (P4) and adult (P60) mice in both back and tail skin, with no staining in the hair follicle, dermis or interfollicular epidermis. Sections from X-gal-stained tissues were counterstained with Eosin. (D) Immunofluorescence staining of β-galactosidase and E-cadherin confirms that Scd3-induced Cre activity is largely limited to differentiated sebocytes. The contour in the β-galactosidase staining (left) outlines the E-cadherin staining. Scale bars: 50 µm in C and 25 µm in D.

Development (2016) 143, 1823-1831 doi:10.1242/dev.132753

(data not shown). Histological examination of Hematoxylin and Eosin (H&E)-stained skin sections revealed no alterations in homozygous mice compared with controls (data not shown) and immunofluorescence staining did not reveal changes in the expression pattern of the epidermal differentiation markers loricrin, K10 and K14 (Fig. S2C). Furthermore, thin layer chromatography showed no quantitative or qualitative changes of hair lipids (Fig. S2D). These data indicate that heterozygous or homozygous *Scd3-Cre* mice do not show a skin phenotype per se; an important prerequisite for employing them as a tool in genetic studies.

KRAS activation enlarges sebaceous glands and increases sebum secretion

We next asked whether *Scd3-Cre* mice are suitable for targeting the SG without affecting other skin compartments such as the epidermis. For this purpose, we crossed *Scd3-Cre* mice with *LSL-Kras*^{G12D} mice, a widely used conditional model of oncogenic KRAS activation (Jackson et al., 2001). At 8 weeks of age, *Scd3-Cre*$^{+/wt}$*Kras*^{G12D} double transgenic mice presented a greasy coat (Fig. 2A). Measurements with a sebumeter confirmed increased sebum production (Fig. 2B). Thin layer chromatography demonstrated increased levels of hair lipids in *Scd3-Cre*$^{+/wt}$*Kras*^{G12D} mice (Fig. 2C) and quantitative densitometric analysis confirmed increased levels of cholesterol esters (CEs), type II wax diesters (WDEs) and free fatty acids (FFAs) compared with *Scd3-Cre*$^{+/wt}$ mice (Fig. 2D). Histologically, *Scd3-Cre*-driven activation of KRAS resulted in considerable enlargement of SGs without affecting epidermal thickness (Fig. 2E). Quantitative morphometry confirmed an increase in SG area (Fig. 2F) but no changes in epidermal thickness in mice with *Scd3-Cre*-induced KRAS activation (Fig. 2G). Accordingly, cell proliferation, assessed as the number of Ki67^{+} cells, was significantly increased in the SGs but unchanged in the epidermis (Fig. 2H).

Interestingly, 50% (3/6) of all examined *Scd3-Cre*$^{+/wt}$*Kras*^{G12D} animals developed single papillomatous outgrowths on their lips (Fig. S3A). Histological analysis showed marked hyperplasia and hyperkeratosis (Fig. S3B), indicating the presence of benign squamous cell papilloma, as reported previously (Caulin et al., 2004). Such tumors might arise from *Scd3-Cre*-induced recombination of the conditional *Kras* allele in SGs on the lip/buccal mucosa border (Fordyce's spots). Alternatively, as the oral mucosa has been demonstrated to be highly susceptible to KRAS-induced oncogenic transformation (van der Weyden et al., 2011), these tumors may be a consequence of spontaneous recombination of the oncogenic *Kras* allele and the oral mucosa of *Scd3-Cre*$^{+/wt}$*Kras*^{G12D} mice.

Scd3-Cre-induced cell ablation depletes differentiated sebocytes and impairs sebum production

To assess the consequences of abolishing sebum production, we next depleted differentiated sebocytes by targeted expression of the diphtheria toxin A chain (DTA). To this purpose we crossed *Scd3-Cre*$^{+/wt}$ mice with mice carrying a conditional *dta* allele placed under the control of the ubiquitously active *Rosa26* promoter

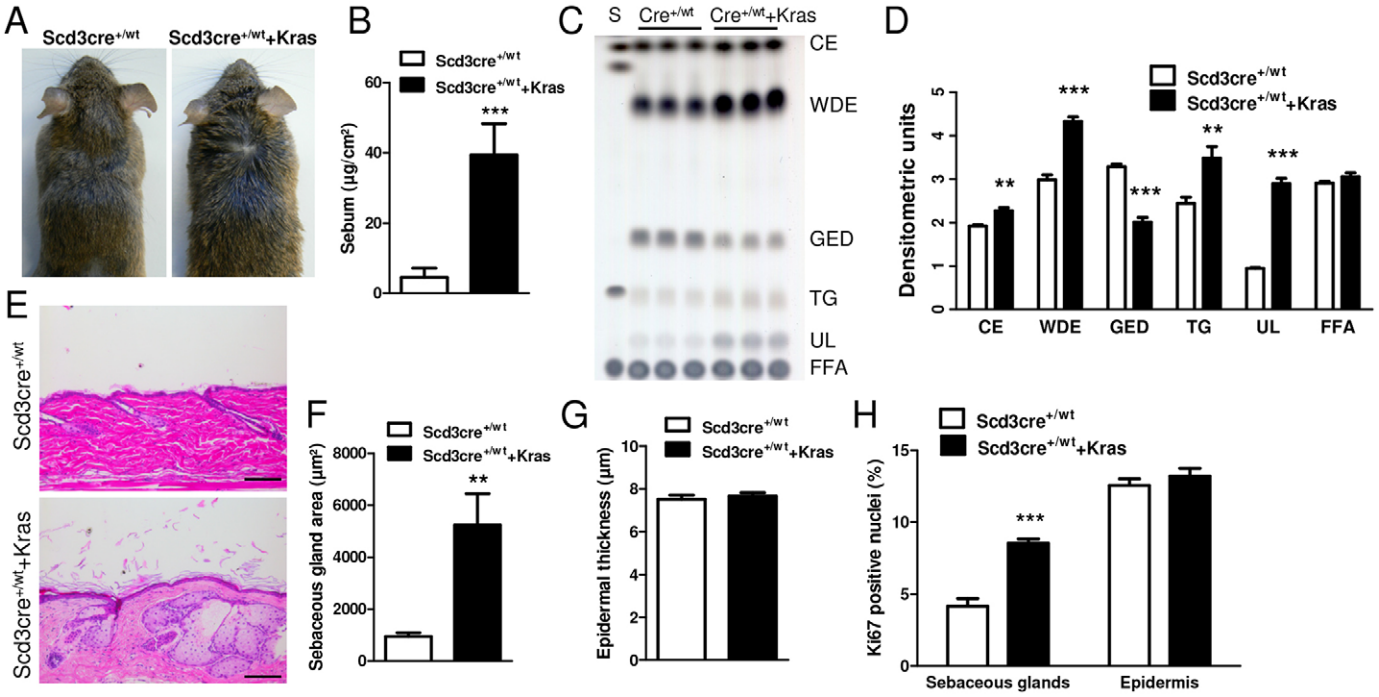

Fig. 2. *Scd3-Cre*-induced KRAS activation increases size and activity of sebaceous glands. (A) Normal hair coat in *Scd3-Cre*$^{+/wt}$ mice and oily hairs in *Scd3-Cre*$^{+/wt}$*Kras*^{G12D} mice. (B) Increased sebum levels in the skin of *Scd3-Cre*$^{+/wt}$*Kras*^{G12D} mice compared with *Scd3-Cre*$^{+/wt}$ mice as evaluated by a sebumeter (n=4 mice/genotype). (C) Thin layer chromatography showing increased amounts of hair lipids in *Scd3-Cre*$^{+/wt}$*Kras*^{G12D} mice compared with *Scd3-Cre*$^{+/wt}$ mice. S, standard lipids; CE, cholesterol esters; WDE, type II wax diesters; GED, glyceryl ether diesters; TG, triglycerides; FFA, free fatty acids; UL, unlabeled. (D) Quantitative densitometric analysis confirmed increased levels of CE, WDE and FFA in *Scd3-Cre*$^{+/wt}$*Kras*^{G12D} mice. (E) H&E-stained back skin sections demonstrate greatly enlarged sebaceous glands in *Scd3-Cre*$^{+/wt}$*Kras*^{G12D} mice compared with *Scd3-Cre*$^{+/wt}$ mice. (F,G) Morphometric analysis confirmed a significant enlargement of the mean sebaceous gland area in *Scd3-Cre*$^{+/wt}$*Kras*^{G12D} mice, but no changes in epidermal thickness compared with *Scd3-Cre*$^{+/wt}$ mice (n=3 mice/genotype). (H) Ki67^{+} nuclei were increased in sebaceous glands in *Scd3-Cre*$^{+/wt}$*Kras*^{G12D} mice, but there were no changes in epidermis compared with *Scd3-Cre*$^{+/wt}$ mice (n=3 mice/genotype). Values are means±s.d. Student's t-test: *P<0.05, **P<0.01, ***P<0.001. Scale bars: 100 µm in E.

Development (2016) 143, 1823-1831 doi:10.1242/dev.132753

(Brockschnieder et al., 2006). *Scd3-Cre*$^{+/wt}$*+DTA* double transgenic mice grew normally and showed a normal hair coat with no signs of alopecia. To assess whether removing hair shafts would evoke any cutaneous abnormality, we shaved *Scd3-Cre*$^{+/wt}$*+DTA* mice at 8 weeks of age and analyzed the skin 6 weeks later. Hair re-growth and skin macroscopic appearance were normal, and histological examination (Giemsa staining, MHC class II immunohistochemical staining) failed to reveal any pathology or increases in the number of inflammatory cells (data not shown). Furthermore, quantitative analysis revealed no changes in the density of hair follicles (Fig. S4A), and there were no changes in hair follicle cycling between *Scd3-Cre*$^{+/wt}$*+DTA* and control mice when this was assessed by quantitative hair cycle histomorphometry around the spontaneous onset of hair follicle cycling during entry into the first catagen phase (at P19.5, Fig. S4B) and the first telogen (at P21.5, Fig. S4C). This finding is interesting in the context of communication between the hair follicle and SG (see Discussion).

Histological examination of H&E-stained back skin and tail skin sections showed that while SGs were still present in *Scd3-Cre*$^{+/wt}$*+DTA* skin, the glands were atrophic and largely lacked differentiated sebocytes (Fig. 3A). Notably, LRIG1^{+} cells, representing an important pool of sebocyte progenitors, appeared normal in the pilosebaceous unit of *Scd3-Cre*$^{+/wt}$*+DTA* mice (Fig. S5). Nile Red staining of back skin cryosections confirmed an almost complete depletion of lipids within the SGs of *Scd3-Cre*$^{+/wt}$*+DTA* mice (Fig. 3B). Thin layer chromatography suggested a reduction in the amount of WDE in the hair lipids of *Scd3-Cre*$^{+/wt}$*+DTA* mice (Fig. 3C) and quantitative densitometric analysis confirmed a significant reduction in the WDE and TG lipid fractions (Fig. 3D). These findings indicate that *Scd3-Cre* mice can be employed for targeting specific pathways of sebaceous lipogenesis.

Loss of sebaceous lipids impairs water repulsion, thermoregulation and resistance against UVB-induced apoptosis

Next, we evaluated whether depletion of differentiated sebocytes affected functions that have been attributed to sebum. To avoid lipid transfer by contact between animals, mice were separated according to their genotype for at least 4 weeks before performing the experiments. First, *Scd3-Cre*$^{+/wt}$ (controls) and *Scd3-Cre* $^{+/wt}$*+DTA* mice at 8 weeks of age were subjected to a water repulsion assay in order to assess their ability to repel water and maintain normal body temperature. Immediately after swimming, *Scd3-Cre*$^{+/wt}$*+DTA* mice looked much wetter than controls and whereas control mice appeared nearly dry after 20 min, *Scd3-Cre*$^{+/wt}$*+DTA* mice were still wet even after 50 min (Fig. 4A). The delayed drying correlated well with a significant increase in water retention during the whole period (Fig. 4B). Both control and *Scd3-Cre*$^{+/wt}$*+DTA* mice had a body temperature of ∼35.2°C before swimming. In control mice, the temperature dropped to 32.8°C immediately after swimming and

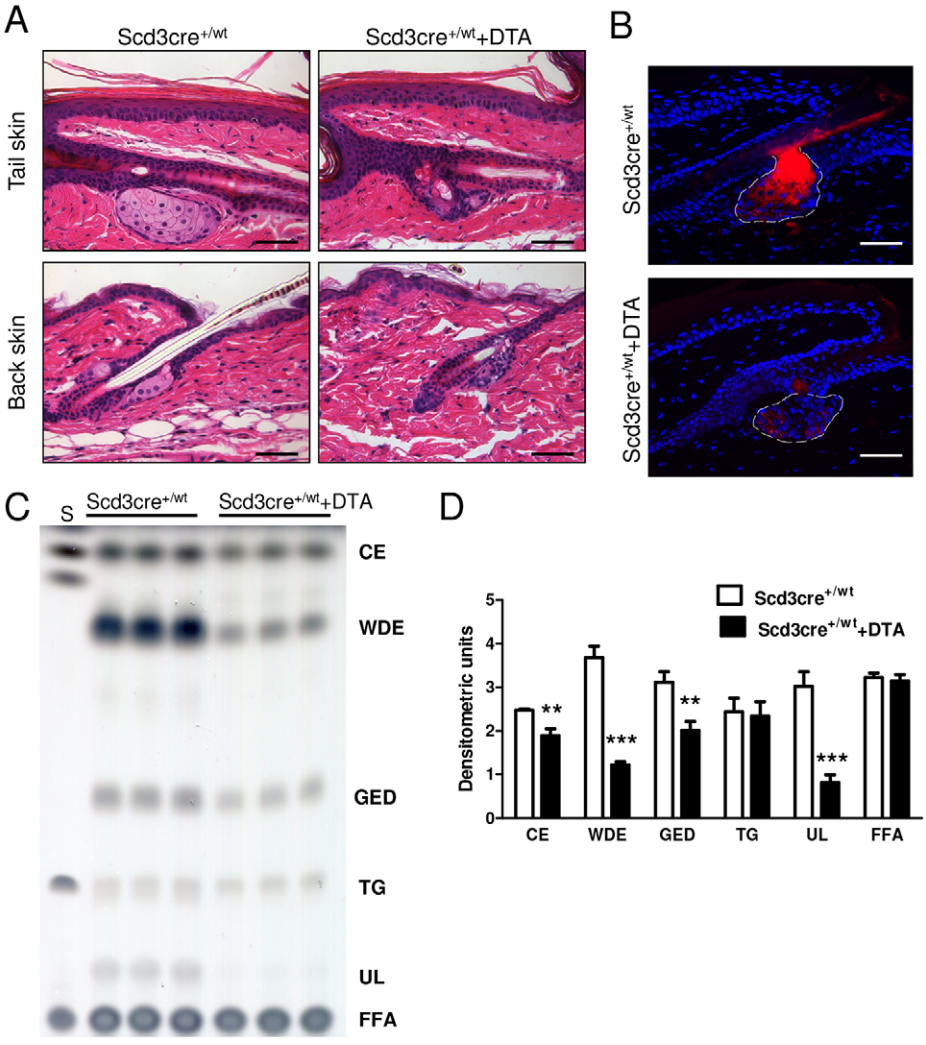

Fig. 3. Ablation of mature sebocytes and depletion of sebaceous lipids in *Scd3-Cre*$^{+/wt}$*+DTA* mice. (A) H&E-stained sections of tail and back skin showing atrophy of sebaceous glands in *Scd3-Cre*$^{+/wt}$*+DTA* mice. (B) Immunofluorescence images of Nile Red-stained back skin show massive loss of sebaceous lipids in *Scd3-Cre*$^{+/wt}$+DTA mice. (C) Thin layer chromatography showing reduced hair lipid amounts in *Scd3-Cre*$^{+/wt}$*+DTA* mice compared with *Scd3-Cre*$^{+/wt}$ mice. S, standard lipids; CE, cholesterol esters; WDE, type II wax diesters; GED, glyceryl ether diesters; TG, triglycerides; FFA, free fatty acids; UL, unlabeled. (D) Quantitative densitometric analysis confirmed reduced levels of WEII and TG in *Scd3-Cre*$^{+/wt}$*+DTA* mice. Values are means±s.d. Student's *t*-test: **P*<0.05, ***P*<0.01. Scale bars: 100 µm in A,B.

Development (2016) 143, 1823-1831 doi:10.1242/dev.132753

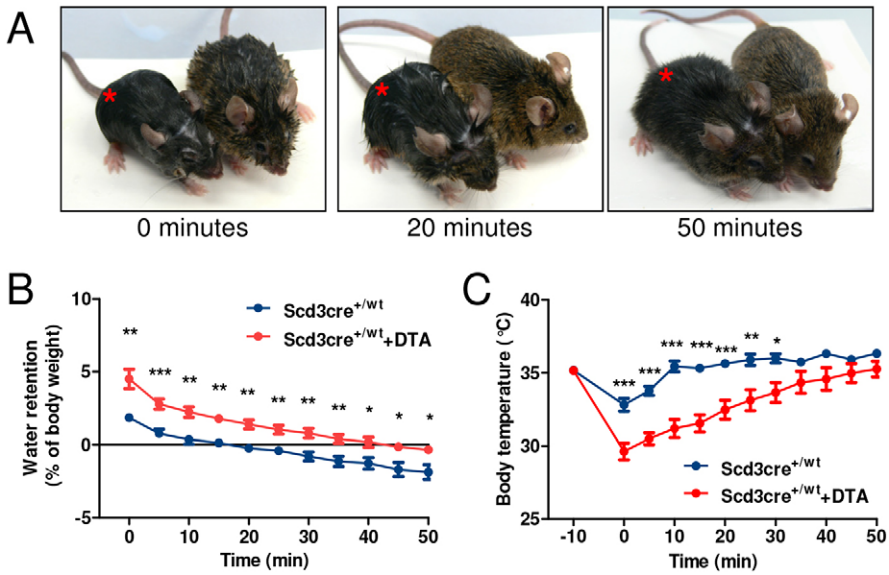

Fig. 4. Water repulsion and thermoregulation are defective in *Scd3-Cre$^{+/wt}$+DTA* mice. (A) Images of animals immediately after (left, 0 min), at 20 min (middle) or at 50 min (right) after immersion in water at 30°C for 2 min. Note the clearly wetter appearance of *Scd3-Cre$^{+/wt}$+DTA* mice (red star) after 20 and 50 min. (B,C) After water immersion, body mass and temperature were measured every 5 min for 50 min. *Scd3-Cre$^{+/wt}$+DTA* mice absorb twice as much water as control mice, show a significantly more accentuated drop in body temperature and need a much longer time to reach normal temperature (n=7 males/genotype). Values are means±s.e.m. Student's t-test: *P<0.05, **P<0.01, ***P<0.001.

returned to the normal value 10 min later (Fig. 4C). By contrast, the temperature of *Scd3-Cre$^{+/wt}$+DTA* mice dropped to 29.6°C immediately after swimming and remained lower than normal for ~30 min (Fig. 4C). Thus, severe depletion of sebaceous lipids significantly affected the ability of *Scd3-Cre$^{+/wt}$+DTA* mice to repel water and to regulate their temperature when wet.

Next, we assessed whether sebaceous lipids are beneficial for the epidermis when it is exposed to UVB irradiation. Twenty-four hours after irradiation of the back skin with UVB, no differences in epidermal thickness (Fig. 5A) or in the percentage of Ki67$^+$ cells (Fig. 5B) were detected between control and *Scd3-Cre$^{+/wt}$+DTA* mice. However, the number of UVB-induced apoptotic cells, measured as the percentage of cleaved caspase-3$^+$ cells (Fig. 5C) or phosphorylated histone γH2AX (Fig. 5D), was significantly increased in *Scd3-Cre$^{+/wt}$+DTA* mice.

These results reveal that sebaceous lipids are essential for water repulsion and thermoregulation, and protect the epidermis against the genotoxic effects of UVB.

Depletion of Meibomian gland sebocytes causes an inflammatory dry eye phenotype

Long-term observation of *Scd3-Cre$^{+/wt}$+DTA* mice revealed an eye disorder that became macroscopically visible from 3 months of age and was characterized by narrow eye fissures, eyeball opacity, frequent blinking and signs of eye inflammation (Fig. 6A). Analysis of H&E-stained sections revealed an almost complete depletion of mature sebocytes in Meibomian glands of *Scd3-Cre$^{+/wt}$+DTA* mice (Fig. 6B) and Nile Red staining confirmed a massive reduction in the lipids synthesized by the gland (Fig. 6C). Histologically, no significant alterations were observed in the cornea at 3 weeks or 2 months of age (Fig. 6D). By contrast, all nine examined *Scd3-Cre$^{+/wt}$+DTA* mice at 8 months of age showed chronic, severe keratoconjunctivitis sicca characterized by hyperkeratinization of the corneal epithelium accompanied by purulent inflammation of secondary origin (Fig. 6D). Thus, *Scd3-Cre* mice will be a useful tool for assessing the functional role of different gene products in Meibomian glands.

Rodents are among the animals possessing Harderian glands, which are located behind the eyeball and produce lipids assumed to be important for fur impregnation and lubrication of the cornea (Payne, 1994). Although β-gal staining revealed widespread Cre expression in the Harderian gland (Fig. S6A), the overall tissue structure (Fig. S6A) and lipid production, as assessed by Nile Red staining (Fig. S6B), remained largely unaltered in *Scd3-Cre$^{+/wt}$+DTA* mice. Some acini presented dilated, with epithelial flattening, loss of lipid droplets and the presence of dark, elongated nuclei (Fig. S6C). However, as these changes were present in only a small proportion of the gland, we conclude that the eye pathology is primarily due to the defects in Meibomian glands, although a minor contribution by the changes in the Harderian gland cannot be excluded.

DISCUSSION

Up to now, regulatory sequences of keratin genes or other structural proteins have been used for targeting genes in the epithelial compartment of the skin. This strategy has the drawback that numerous cell types in the epidermis and in the pilosebaceous unit are targeted in parallel, potentially causing side effects and

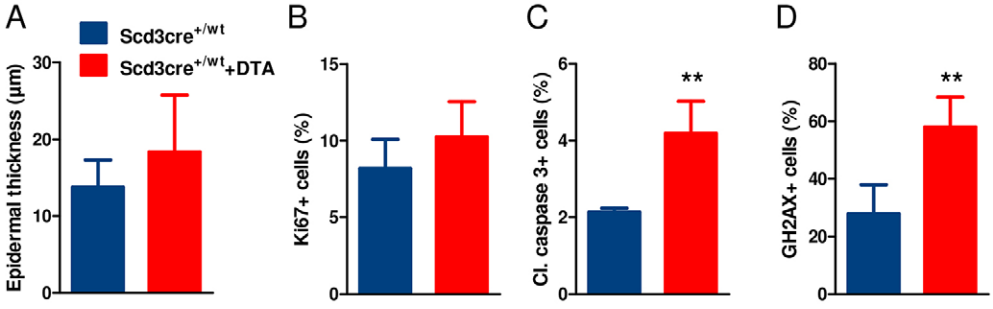

Fig. 5. Protection against UVB-induced apoptosis is impaired in *Scd3-Cre$^{+/wt}$+DTA* mice. Animals (n=4 males/group) were anesthetized and the shaved back skin was irradiated with 200 mJ/cm^2 UVB (280-320 nm) Mice were sacrificed 24 h after irradiation and the epidermal thickness (A), the number of Ki67$^+$ cells (B), the number of cleaved caspase-3$^+$ cells (C) and the number of phosphorylated γH2AX$^+$ cells (D) were assessed. Values are means±s.d. Student's t-test: **P<0.01.

Development (2016) 143, 1823-1831 doi:10.1242/dev.132753

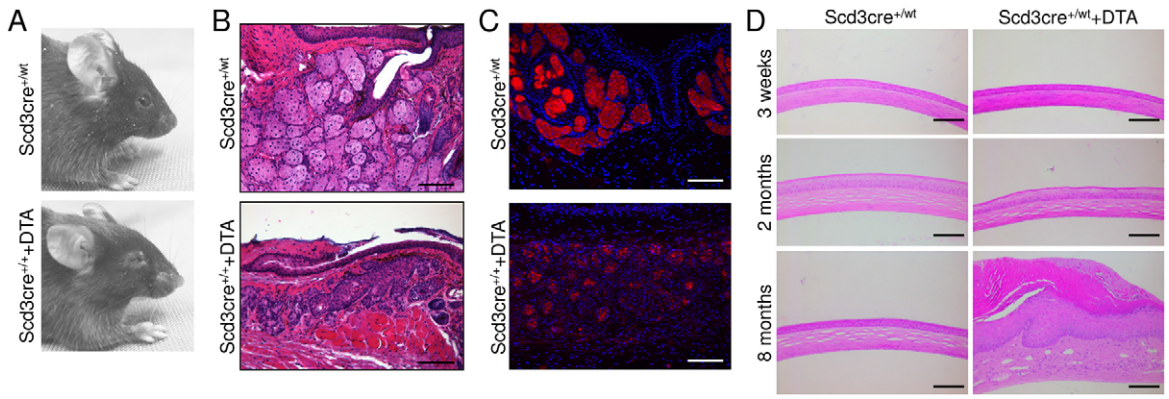

Fig. 6. Eye pathology resembling human Meibomian gland disorder in *Scd3-Cre$^{+/wt}$+DTA* mice. (A) Gross eye phenotype of *Scd3-Cre$^{+/wt}$+DTA* and control mice. Control eyes are rounded, whereas those of *Scd3-Cre$^{+/wt}$*+DTA mice have an elongated profile. (B) H&E-stained sections showing atrophic Meibomian glands in *Scd3-Cre$^{+/wt}$+DTA* mice. (C) Fluorescent images of Nile Red-stained sections reveal a severe depletion of lipids in the Meibomian gland of *Scd3-Cre$^{+/wt}$+DTA* mice. (D) Histological appearance (H&E staining) showing hyperkeratosis of the corneal epithelium and accumulation of purulent masses on the cornea of *Scd3-Cre$^{+/wt}$+DTA* mice at 8 months of age. Scale bars: 100 µm in B,C and 200 µm in D.

unspecific phenotypes. In the present study, we employed the *Scd3* genomic locus to create a *Cre*-expressing mouse line that allows gene targeting specifically in sebocytes. Faithful expression of *Cre* in hair follicle-associated and 'free' SGs was demonstrated by RT-PCR and by breeding into the *lacZ* reporter background (Soriano, 1999). In addition, *Scd3-Cre*-mediated activation of oncogenic KRAS, by breeding into the *Kras^{G12D}* background, (Jackson et al., 2001) resulted in phenotypical changes restricted to the SG, thus confirming the functionality and specificity of the developed tool. Although we observed a weak and patchy recombination in the intestinal epithelium and in the brain, this did not seem to have any consequence, and no phenotypical changes were observed in these sites in *Scd3-Cre$^{+/wt}$Kras^{G12D}* mice. Furthermore, loss of *Scd3* expression in *Scd3-Cre$^{+/+}$* mice did not cause any detectable phenotypical change, indicating that this line can be reliably employed in heterozygous and also probably in homozygous state without the risk of creating an 'own' phenotype.

Sebaceous lipids have been traditionally associated with skin and hair coat waterproofing in animals. The *in vitro* antioxidant and antimicrobial properties of sebum led to the suggestion that it might have other protective roles beyond waterproofing, but this view has also been strongly contested (Kligman, 1963). One important complicating factor is that for most available genetic models, loss of sebum is accompanied by loss of epidermal lipids. To obtain a model lacking specifically sebum lipids but preserving epidermal lipids, we employed a cell ablation strategy in which *Scd3-Cre* mice were bred with a mouse line allowing Cre-mediated activation of DTA (Brockschnieder et al., 2006). This resulted in considerable depletion of mature sebocytes, greatly impaired SG lipid content and a significant depletion of WE and TG in hair lipids. Together, WE and TG make up roughly 50% of lipid species in mouse hair (Lin et al., 2013). Considering the extensive ablation of mature sebocytes and the almost complete absence of lipids within the SG, it remains unclear why the chromatography did not reveal an even stronger reduction in overall hair lipids. Possibly, the hair shafts are able to bind and accumulate SG-derived lipids, thus masking an even lower lipid production from targeted SGs.

Although almost completely lacking mature sebocytes and sebum secretion, *Scd3-Cre$^{+/wt}$+DTA* mice displayed a normal hair coat without signs of inflammation or alopecia and normal spontaneous hair follicle cycling. This is initially surprising, as previous mouse lines with SG deficiency, including the classic *asebia* mutant (Schneider, 2015) and numerous mouse lines with targeted mutations in genes such as *Sox9* (Vidal et al., 2005), *Dgat1* (Chen et al., 2002) or *Scd1* (the *asebia*-associated gene; Miyazaki et al., 2001), commonly present with alopecia or at least severe pathological changes of the hair follicle. In fact, although SGs can form and function in the absence of a hair follicle, the latter might neither form nor function normally in the absence of an SG (Stenn et al., 2008). For instance, it has long been recognized that the SG is required for the successful separation of the hair shaft from the inner root sheath (Gemmell and Chapman, 1971; Straile, 1965; Williams et al., 1996; Williams and Stenn, 1994), and disruption of this interaction appears to be the reason for alopecia in asebia mice (Sundberg et al., 2000). Moreover, SG-controlled lipid production has been postulated to be a major control element of hair follicle biology (Stenn and Karnik, 2010). In *Scd3-Cre$^{+/wt}$+DTA* mice, however, SGs are not lost but rather lack mature, lipid-filled sebocytes, reflecting the fact that SCD3 is expressed in differentiated sebocytes only (Zheng et al., 2001). Furthermore, LRIG1^{+} sebocyte progenitors are maintained in the pilosebaceous unit of *Scd3-Cre$^{+/wt}$+DTA* mice. Thus, our results suggest that rather than sebum, the structural presence of an SG might be required for shaft-sheath interactions.

That *Scd3-Cre$^{+/wt}$+DTA* mice show no hair cycle abnormality, at least during the investigated crucial hair cycle time points, is also of interest in a different context. It has long been recognized that SG gland size/volume (Chase et al., 1953) and defined SG activities such as alkaline phosphatase activity (Handjiski et al., 1994) and the expression of key proteins involved in cutaneous retinoic acid synthesis and signaling (Everts et al., 2007), significantly change in association of the cyclic activity of the hair follicle. It has long been an open and controversially discussed question whether the cycling hair follicle induces and controls these SG changes, or whether, vice versa, the SG actually impacts hair follicle cycling. While the current study cannot resolve this quandary, our observation that the hair follicle appears unaffected, even by the loss of one of the key functions of the SG, i.e. lipid production and secretion, could be interpreted to suggest that it is in fact the hair follicle that controls hair cycle-associated changes in SG biology.

Notably, sebum depletion negatively influenced the ability of mice to repulse water and increased their susceptibility to UVB-

Development (2016) 143, 1823-1831 doi:10.1242/dev.132753

induced apoptosis. After swimming in 30°C water for 2 min, *Scd3-Cre*$^{+/wt}$*+DTA* mice displayed severe defects in repelling water and in regulating their body temperature. While several additional factors, including hair coat, skin blood circulation and regulation by the central nervous system, contribute to thermoregulation, it is likely that the observed defects are the result of depletion of sebum wax esters, which might lead to increased sebum fluidity and impaired fur waterproofing. Defects in water repulsion and thermoregulation have been previously described in several mouse lines lacking proteins involved in lipid synthesis (Chen et al., 2002; Lin et al., 2013; Westerberg et al., 2004; Zhang et al., 2014). However, in all mouse lines previously assessed, the defect was also present in the epidermis, making it impossible to discern between the roles played by epidermal and sebaceous lipids. Thus, to the best of our knowledge, the current study is the first to demonstrate that sebaceous lipids have an essential role in regulating water repulsion and thermoregulation that cannot be compensated by epidermal lipids. Furthermore, after UVB irradiation, the percentage of cleaved caspase-3^{+} cells or phosphorylated histone γH2AX, a highly sensitive marker for the analysis of UVB-induced apoptosis (Barnes et al., 2010), were significantly increased in *Scd3-Cre*$^{+/wt}$*+DTA* mice. Although these results reveal a protective role of sebaceous lipids against the genotoxic effects of UVB in the mouse epidermis, future studies addressing the underlying mechanisms will be needed.

In addition to the hair follicle (Schneider et al., 2009), sebocytes are found at several other locations of the body forming so-called free or ectopic SGs. An eminent example is the Meibomian glands, which reside within the tarsal plate of both the upper and lower eyelid (Knop et al., 2011). The glandular acini secrete lipids (meibum) onto the ocular surface, where they contribute to the maintenance and structural integrity of the tear film. We noticed that *Scd3-Cre*$^{+/wt}$*+DTA* mice aged 3 months or older displayed narrow eye fissures, eyeball opacity, frequent blinking and signs of eye inflammation. Such a phenotype can have different causes, including palpebral edema or corneal diseases. However, the presence of dystrophic Meibomian glands, hyperkeratinization and secondary inflammatory lesions of the cornea indicate loss of meibum as a pathogenic mechanism behind the observed keratoconjunctivitis (although a minor contribution by a deficit in Harderian gland secretion cannot be excluded). This condition resembles Meibomian gland disorder (MGD), which represents a significant part of dry eye disease, a chronic disorder that affects millions of people each year (Knop et al., 2011; Nelson et al., 2011). Owing to anatomical similarities, mice are a popular model for studying the pathogenesis of MGD. Furthermore, mouse meibum lipid composition strongly resembles that of humans (Butovich et al., 2012) and mouse Meibomian glands show an age-related atrophy that mimics changes seen in age-related MGD (Jester et al., 2011). MGD has been studied in mice exposed to a desiccating environment (Suhalim et al., 2014) or in diverse genetically modified mice lacking enzymes or transcription factors important for sebaceous lipid synthesis (House et al., 2010; McMahon et al., 2014; Yagyu et al., 2000). In particular, the dry eye phenotype observed in *Scd3-Cre*$^{+/wt}$*+DTA* mice shows striking similarities to the ocular disease in Tabby mice, a line carrying a mutation in the ectodysplasin A gene (Cui et al., 2005). In the future, *Scd3-Cre* will be useful for analyzing the function of numerous gene products and of defined lipid species in tear film physiology by eliminating them specifically in meibocytes.

In summary, our results indicate that *Scd3-Cre* mice can be successfully used to drive recombination specifically in sebocytes. This new mouse line will therefore permit, for the first time, assessment of the specific roles of sebaceous lipids without confounding influences from the concomitant loss of epidermal lipids. Thus, we are confident that this new tool will significantly expand the experimental armory for studying the roles of sebaceous lipids in health and disease. Initial studies carried out in a mouse line with severely compromised terminal differentiation of sebocytes and impaired sebum production confirmed an important role for sebum in repelling water and regulating body temperature after water immersion and in protecting epidermal cells against UVB-induced apoptosis. Sebaceous lipids from the Meibomian gland were also essential for generating a functional tear film and for the integrity of the eye surface. These mice might therefore represent an important model for studying the pathogenesis and possible therapeutic strategies of Meibomian gland dysfunction in humans.

MATERIALS AND METHODS

Animals

Rosa26-LacZ reporter mice (Soriano, 1999), *LSL-Kras*^{G12D} (Jackson et al., 2001) and *Rosa26-DTA* (Brockschnieder et al., 2006) were described previously. For generating *Scd3-Cre* mice, we employed the pPNT4 plasmid (Conrad et al., 2003) to generate a targeting vector to knock in a codon-improved Cre recombinase cDNA (Shimshek et al., 2002) immediately before the first ATG in exon 1 of the mouse *Scd3* gene. E14 mouse embryonic stem cells were electroporated with 35 µg of the *Sal*I-linearized vector using 0.8 kV and 3 µFD in a Gene Pulser II (Bio-Rad). After selection with G418 for 1 week, resistant clones were picked, expanded and aliquots were frozen or further expanded for DNA isolation. Homologous recombination was detected by standard PCR using one vector-based and one external primer each at both 5′ and 3′ ends. For generating mice, embryonic stem cells carrying the targeted allele (clone A10) were injected into C57BL/6N blastocysts and transferred to pseudopregnant NMRI foster mothers. The resulting chimeras were crossed to C57BL/6N mice to produce mice heterozygous for the mutation.

Mice were maintained under specific pathogen-free conditions and had access to water and standard rodent diet (V1534, Ssniff, Soest, Germany) *ad libitum*. All experiments were approved by the Committee on Animal Health and Care of the local governmental body of the state of Upper Bavaria (Regierung von Oberbayern) and performed in strict compliance with the European Communities Council Directive (86/609/EEC) recommendations for the care and use of laboratory animals.

In vivo experiments

Epidermal sebum levels were measured with a sebumeter (SM810, Courage and Khazaka, Cologne, Germany). For UVB irradiation, animals were anesthetized and the shaved back skin was irradiated with 200 mJ/cm^2 UVB (280-320 nm) using a Medisun HF-144 apparatus (Schulz & Böhm, Brühl, Germany). Mice were sacrificed 24 h after skin irritation. For the water retention and thermoregulation assay, mice were allowed to swim or float in water at 30°C for 2 min and excessive water was eliminated by briefly putting them on paper towels. Body mass and rectal temperature (Thermometer from Testo, Lenzkirch, Germany) were recorded 10 min before, immediately after and then every 5 min after water immersion. The hair water content was calculated by subtracting the body mass before immersion from the mass after immersion.

Morphometric analysis

Quantitative histomorphometry was performed using morphologic criteria to determine the different HF cycle phases on P19.5 and P21.5 (Müller-Röver et al., 2001). For the quantitative evaluation of epidermal and dermal thickness, HF numbers, SG area and proliferation index, two different sections from the back skin of each animal were stained with H&E. Pictures covering a length of 13 mm of epidermis (distributed over a total length of 5.2 cm of back skin) were taken with a 200× magnification lens using a Leica DFC425C digital camera per animal to be measured. Epidermal and dermal thickness was investigated on the same sections on 10 constantly

Development (2016) 143, 1823-1831 doi:10.1242/dev.132753

distributed measuring points per picture, resulting in a total of 200 measuring points per animal. For determining the sebaceous gland proliferation rate, the total number of cells and the number of proliferating cells per gland was determined on the same samples after staining for Ki67. To analyze the epidermal proliferation rate, apoptosis rate and proportion of $\gamma H2AX^+$ nuclei, the total number of epidermal nuclei and the total number of Ki67, cleaved caspase-3^+ and $\gamma H2AX^+$ nuclei were counted. The number of HFs was recorded and area of all visible SGs was recorded with LAS Software v.3.8.0 (Leica Microsystems), which was also used to calculate the mean gland area.

Histology, immunohistochemistry and immunofluorescence

After euthanasia, skin samples were fixed in 4% paraformaldehyde (PFA, Sigma) or 95% ethanol with 1% acetic acid, dehydrated, and embedded in paraffin or directly snap-frozen and stored at −80°C. Hematoxylin and Eosin-stained sections were used for histological analysis. For the detection of proliferating cells, apoptotic cells and DNA strand breaks, immunohistochemical staining of Ki67, cleaved caspase-3 and γH2AX were performed. Briefly, sections were boiled for antigen retrieval in 10 mM sodium citrate buffer (pH 6.0) and the endogenous peroxidase was blocked with 3% H_2O_2 for 15 min. Slides were blocked with 5% rabbit serum and incubated overnight at 4°C with a rat anti-Ki67 antibody (DAKO, M7248) diluted 1:200. After washing in Tris-buffered saline solution (TBS), the slides were incubated for 1 h with a secondary biotin-conjugated rabbit anti-rat antibody (DAKO) diluted 1:200 and then for 30 min with streptavidin-biotin complex. 3,3′-diaminobenzidine (KEM-EN-TEC, Taastrup, Denmark) was used as a chromogen. For apoptosis staining and for the detection of DNA strand breaks the procedure was similar to the previous Ki67 staining. The only difference was that the slides were boiled in 10 mM sodium citrate buffer (pH 6.0) for 35 min in a pressure cooker for antigen retrieval and were blocked with 5% goat serum. The following antibodies were used: rabbit anti-cleaved caspase-3 (Cell Signaling, 9661, 1:200), rabbit anti-γH2AX (pSer139) (Novus Biologicals, NB100-384, 1:200) and goat anti-rabbit (Vector Laboratories, BA-1000, 1:200).

Epidermal differentiation was investigated by immunofluorescence analysis. Briefly, acetic ethanol-fixed sections were blocked with 3% BSA in PBS, 1% Tween (PBST) and incubated overnight at 4°C with rabbit anti-keratin 10 (Covance, PRB-159P, 1:500), anti-keratin 14 (Covance, PRB-155P, 1:50,000) or anti-loricrin antibody (Covance, PRB-145P, 1:250) in blocking solution. Then, slides were washed with PBST and incubated with goat anti-rabbit Cy3 antibody (1:250) (Jackson ImmunoResearch) and Hoechst 33342 (1:1000) (Sigma) in blocking solution for 2 h at room temperature (RT). After washing with PBS, the sections were mounted with Mowiol, 10% DABCO (Sigma).

Nile Red staining was performed on 8 µm cryosections. Sections were fixed for 10 min in 4% paraformaldehyde and washed twice for 5 min in TBS. Slides were incubated with Nile Red solution (1:100) (AdipoRed, Lonza, Basel, Switzerland) for 5 min and then washed twice for 5 min in TBS. For immunofluorescence staining, cryosections were incubated for 2 h at RT with the following primary antibodies: rabbit anti-SCD3 (LifeSpan BioSciences, LS-C39249, 1:100); rabbit anti-β-galactosidase (Novus Biologicals, NB600-305, 1:100); goat anti-LRIG1 (R&D Systems, AF3688, 1:100); goat anti-E-cadherin (R&D Systems, AF748, 1:100). Sections were then washed and incubated with an appropriate secondary antibody labeled with Alexa Fluor 594 or Alexa Fluor 488 (Dianova, Hamburg, Germany). All sections were mounted with Vectashield (Vector Laboratories) with DAPI and stored at 4°C.

For β-gal staining, the organs of *Rosa26-lacZ+Scd3-Cre* and *Rosa26-lacZ* mice were fixed in phosphate-buffered saline (PBS) containing 0.02% NP-40, 1% formaldehyde and 0.2% glutaraldehyde at 4°C for 2 h, washed twice with PBS for 20 min at RT and incubated overnight at RT under careful shaking in staining solution (0.02% NP-40, 2 mM $MgCl_2$, 5 mM $K_3Fe(CN)_6$ and 5 mM $K_4Fe(CN)_6$•$3H_2O$, 0.01% sodium deoxycholate, and 1 mg/ml X-gal in PBS, pH 7.4). After staining, samples were washed in PBS as above and post-fixed in PBS with 4% paraformaldehyde, routinely processed and embedded in paraffin blocks. Histological sections were stained with Eosin.

RNA expression analysis

Tissue samples were homogenized in TRIzol (Invitrogen) for RNA isolation and 2 µg of RNA was reverse-transcribed in a final volume of 20 µl using RevertAid Reverse Transcriptase (Thermo Scientific) according to the manufacturer's instructions. For qualitative mRNA expression of *Scd3*, *Gapdh* and *Cre*, a RT-PCR using reagents from Qiagen (Hilden, Germany) was performed. The final reaction volume was 20 µl, and cycle conditions were 94°C for 5 min, followed by 35 cycles of 94°C for 1 min, 60°C for 1 min and 72°C for 1 min. The primers employed were: *Scd3* forward primer, 5′-GCTGCAAGAAGAGATGAC-GCC-3′ and reverse primer, 5′-CAATGCCCTCAATACTGATCACA-3′; *Cre* forward primer, 5′-GGCAGGCCTTCTCTGAACA-3′ and reverse primer, 5′-GGAAGGCCAGGTTCCTGAT-3′; and *Gapdh* forward primer, 5′-TCATCAACGGGAAGCCCATCAC-3′ and reverse primer, 5′-AGAC-TCCACGACATACTCAGCACCG-3′.

Thin layer chromatography

Sebum was extracted from 50 mg hair with three consecutive extractions with 2 ml chloroform/methanol (2:1). Unified extracts were dried under nitrogen and dissolved in 100 µl acetone/methanol/isopropanol mixture (40:40:20). To separate the lipid extracts, HPTLC silica gel 60 plates 20×10 cm (Merck, Darmstadt, Germany) were used as the stationary phase. 10 µl of the concentrated lipid extract from each sample were loaded onto the HPTLC plate. The separation was achieved by running the HPTLC in benzene/hexane (70:30 v/v). The plates were dried and dyed with a 10% solution of copper sulfate in water/methanol (80:20 v/v). The plates were charred at 120°C for 30 min to develop gray-to-black spots. Densitometry of the developed spots was performed to assess spot intensities using the ImageJ software package (http://imagej.nih.gov/ij/).

Statistical analysis

Data were analyzed using the Student's *t*-test (GraphPad Prism) and are presented as means±s.d. except for the data in Fig. 4B,C and Fig. S4A,B, which were presented as means±s.e.m. $P<0.05$ was considered statistically significant.

Acknowledgements

We appreciate the expert veterinary care provided by Dr Ingrid Renner-Müller and the excellent technical assistance of Petra Renner (animal facility), Matteo Ludovici (lipid analysis) and Stefanie Riesemann (genotyping and expression studies).

Competing interests

The authors declare no competing or financial interests.

Author contributions

M.D., E.C., M.S., A.F. and M.R.S. performed the experiments; M.D., E.C., D.E., R.P. and M.R.S. analyzed the data; D.R. and R.P. provided essential reagents; M.R.S. designed the experiments and wrote the manuscript.

Funding

This research received no specific grant from any funding agency in the public, commercial, or not-for-profit sectors.

Supplementary information

Supplementary information available online at
http://dev.biologists.org/lookup/suppl/doi:10.1242/dev.132753/-/DC1

References

Barnes, L., Dumas, M., Juan, M., Noblesse, E., Tesniere, A., Schnebert, S., Guillot, B. and Molès, J.-P. (2010). GammaH2AX, an accurate marker that analyzes UV genotoxic effects on human keratinocytes and on human skin. *Photochem. Photobiol.* **86**, 933-941.

Brockschnieder, D., Pechmann, Y., Sonnenberg-Riethmacher, E. and Riethmacher, D. (2006). An improved mouse line for Cre-induced cell ablation due to diphtheria toxin A, expressed from the Rosa26 locus. *Genesis* **44**, 322-327.

Butovich, I. A., Lu, H., McMahon, A. and Eule, J. C. (2012). Toward an animal model of the human tear film: biochemical comparison of the mouse, canine, rabbit, and human meibomian lipidomes. *Invest. Ophthalmol. Vis. Sci.* **53**, 6881-6896.

Caulin, C., Nguyen, T., Longley, M. A., Zhou, Z., Wang, X.-J. and Roop, D. R. (2004). Inducible activation of oncogenic K-ras results in tumor formation in the oral cavity. *Cancer Res.* **64**, 5054-5058.

Development (2016) 143, 1823-1831 doi:10.1242/dev.132753

Chase, H. B., Montagna, W. and Malone, J. D. (1953). Changes in the skin in relation to the hair growth cycle. *Anat. Rec.* **116**, 75-81.
Chen, H. C., Smith, S. J., Tow, B., Elias, P. M. and Farese, R. V., Jr (2002). Leptin modulates the effects of acyl CoA:diacylglycerol acyltransferase deficiency on murine fur and sebaceous glands. *J. Clin. Invest.* **109**, 175-181.
Conrad, M., Brielmeier, M., Wurst, W. and Bornkamm, G. W. (2003). Optimized vector for conditional gene targeting in mouse embryonic stem cells. *Biotechniques* **34**, 1136-1138, 1140.
Cui, C.-Y., Smith, J. A., Schlessinger, D. and Chan, C.-C. (2005). X-linked anhidrotic ectodermal dysplasia disruption yields a mouse model for ocular surface disease and resultant blindness. *Am. J. Pathol.* **167**, 89-95.
Everts, H. B., Sundberg, J. P., King, L. E., Jr and Ong, D. E. (2007). Immunolocalization of enzymes, binding proteins, and receptors sufficient for retinoic acid synthesis and signaling during the hair cycle. *J. Invest. Dermatol.* **127**, 1593-1604.
Gemmell, R. T. and Chapman, R. E. (1971). Formation and breakdown of the inner root sheath and features of the pilary canal epithelium in the wool follicle. *J. Ultrastruct. Res.* **36**, 355-366.
Handjiski, B. K., Eichmuller, S., Hofmann, U., Czarnetzki, B. M. and Paus, R. (1994). Alkaline phosphatase activity and localization during the murine hair cycle. *Br. J. Dermatol.* **131**, 303-310.
Hinde, E., Haslam, I. S., Schneider, M. R., Langan, E. A., Kloepper, J. E., Schramm, C., Zouboulis, C. C. and Paus, R. (2013). A practical guide for the study of human and murine sebaceous glands in situ. *Exp. Dermatol.* **22**, 631-637.
House, J. S., Zhu, S., Ranjan, R., Linder, K. and Smart, R. C. (2010). C/EBPalpha and C/EBPbeta are required for Sebocyte differentiation and stratified squamous differentiation in adult mouse skin. *PLoS ONE* **5**, e9837.
Jackson, E. L., Willis, N., Mercer, K., Bronson, R. T., Crowley, D., Montoya, R., Jacks, T. and Tuveson, D. A. (2001). Analysis of lung tumor initiation and progression using conditional expression of oncogenic K-ras. *Genes Dev.* **15**, 3243-3248.
Jester, B. E., Nien, C. J. Y., Winkler, M., Brown, D. J. and Jester, J. V. (2011). Volumetric reconstruction of the mouse meibomian gland using high-resolution nonlinear optical imaging. *Anat. Rec.* **294**, 185-192.
Kligman, A. M. (1963). The uses of sebum. *Br. J. Dermatol.* **75**, 307-319.
Knop, E., Knop, N., Millar, T., Obata, H. and Sullivan, D. A. (2011). The international workshop on meibomian gland dysfunction: report of the subcommittee on anatomy, physiology, and pathophysiology of the meibomian gland. *Invest. Ophthalmol. Vis. Sci.* **52**, 1938-1978.
Lin, M.-H., Hsu, F.-F. and Miner, J. H. (2013). Requirement of fatty acid transport protein 4 for development, maturation, and function of sebaceous glands in a mouse model of ichthyosis prematurity syndrome. *J. Biol. Chem.* **288**, 3964-3976.
McMahon, A., Lu, H. and Butovich, I. A. (2014). A role for ELOVL4 in the mouse meibomian gland and sebocyte cell biology. *Invest. Ophthalmol. Vis. Sci.* **55**, 2832-2840.
Miyazaki, M., Man, W. C. and Ntambi, J. M. (2001). Targeted disruption of stearoyl-CoA desaturase1 gene in mice causes atrophy of sebaceous and meibomian glands and depletion of wax esters in the eyelid. *J. Nutr.* **131**, 2260-2268.
Müller-Röver, S., Foitzik, K., Paus, R., Handjiski, B., van der Veen, C., Eichmüller, S., McKay, I. A. and Stenn, K. S. (2001). A comprehensive guide for the accurate classification of murine hair follicles in distinct hair cycle stages. *J. Invest. Dermatol.* **117**, 3-15.
Neess, D., Bek, S., Bloksgaard, M., Marcher, A.-B., Faergeman, N. J. and Mandrup, S. (2013). Delayed hepatic adaptation to weaning in ACBP−/− mice is caused by disruption of the epidermal barrier. *Cell Rep.* **5**, 1403-1412.
Nelson, J. D., Shimazaki, J., Benitez-del-Castillo, J. M., Craig, J. P., McCulley, J. P., Den, S. and Foulks, G. N. (2011). The international workshop on meibomian gland dysfunction: report of the definition and classification subcommittee. *Invest. Ophthalmol. Vis. Sci.* **52**, 1930-1937.
Payne, A. P. (1994). The harderian gland: a tercentennial review. *J. Anat.* **185**, 1-49.
Sampath, H., Flowers, M. T., Liu, X., Paton, C. M., Sullivan, R., Chu, K., Zhao, M. and Ntambi, J. M. (2009). Skin-specific deletion of stearoyl-CoA desaturase-1 alters skin lipid composition and protects mice from high fat diet-induced obesity. *J. Biol. Chem.* **284**, 19961-19973.
Schneider, M. R. (2012). Genetic mouse models for skin research: strategies and resources. *Genesis* **50**, 652-664.
Schneider, M. R. (2015). Fifty years of the asebia mouse: origins, insights and contemporary developments. *Exp. Dermatol.* **24**, 340-341.
Schneider, M. R. and Paus, R. (2010). Sebocytes, multifaceted epithelial cells: lipid production and holocrine secretion. *Int. J. Biochem. Cell Biol.* **42**, 181-185.
Schneider, M. R., Schmidt-Ullrich, R. and Paus, R. (2009). The hair follicle as a dynamic miniorgan. *Curr. Biol.* **19**, R132-R142.
Shimshek, D. R., Kim, J., Hübner, M. R., Spergel, D. J., Buchholz, F., Casanova, E., Stewart, A. F., Seeburg, P. H. and Sprengel, R. (2002). Codon-improved Cre recombinase (iCre) expression in the mouse. *Genesis* **32**, 19-26.
Smith, K. R. and Thiboutot, D. M. (2008). Thematic review series: skin lipids. Sebaceous gland lipids: friend or foe? *J. Lipid Res.* **49**, 271-281.
Soriano, P. (1999). Generalized lacZ expression with the ROSA26 Cre reporter strain. *Nat. Genet.* **21**, 70-71.
Stenn, K. S. and Karnik, P. (2010). Lipids to the top of hair biology. *J. Invest. Dermatol.* **130**, 1205-1207.
Stenn, K. S., Zheng, Y. and Parimoo, S. (2008). Phylogeny of the hair follicle: the sebogenic hypothesis. *J. Invest. Dermatol.* **128**, 1576-1578.
Straile, W. E. (1965). Root-sheath dermal papilla relationships and the control of hair growth. In *Biology of the Skin and Hair Growth* (ed. A. G. Lyne and B. F. Short), pp. 35-57. Sydney: Angus and Robertson.
Suhalim, J. L., Parfitt, G. J., Xie, Y., De Paiva, C. S., Pflugfelder, S. C., Shah, T. N., Potma, E. O., Brown, D. J. and Jester, J. V. (2014). Effect of desiccating stress on mouse meibomian gland function. *Ocul. Surf.* **12**, 59-68.
Sundberg, J. P., Boggess, D., Sundberg, B. A., Eilertsen, K., Parimoo, S., Filippi, M. and Stenn, K. (2000). Asebia-2J (Scd1(ab2J)): a new allele and a model for scarring alopecia. *Am. J. Pathol.* **156**, 2067-2075.
Thody, A. J. and Shuster, S. (1989). Control and function of sebaceous glands. *Physiol. Rev.* **69**, 383-416.
Tóth, B. I., Oláh, A., Szöllősi, A. G., Czifra, G. and Bíró, T. (2011). "Sebocytes' makeup": novel mechanisms and concepts in the physiology of the human sebaceous glands. *Pflugers Arch.* **461**, 593-606.
van der Weyden, L., Alcolea, M. P., Jones, P. H., Rust, A. G., Arends, M. J. and Adams, D. J. (2011). Acute sensitivity of the oral mucosa to oncogenic K-ras. *J. Pathol.* **224**, 22-32.
Vidal, V. P. I., Chaboissier, M.-C., Lützkendorf, S., Cotsarelis, G., Mill, P., Hui, C.-C., Ortonne, N., Ortonne, J.-P. and Schedl, A. (2005). Sox9 is essential for outer root sheath differentiation and the formation of the hair stem cell compartment. *Curr. Biol.* **15**, 1340-1351.
Westerberg, R., Tvrdik, P., Unden, A.-B., Mansson, J.-E., Norlen, L., Jakobsson, A., Holleran, W. H., Elias, P. M., Asadi, A., Flodby, P. et al. (2004). Role for ELOVL3 and fatty acid chain length in development of hair and skin function. *J. Biol. Chem.* **279**, 5621-5629.
Williams, D. and Stenn, K. S. (1994). Transection level dictates the pattern of hair follicle sheath growth in vitro. *Dev. Biol.* **165**, 469-479.
Williams, D., Siock, P. and Stenn, K. (1996). 13-cis-Retinoic acid affects sheath-shaft interactions of equine hair follicles in vitro. *J. Invest. Dermatol.* **106**, 356-361.
Williams, H. C., Dellavalle, R. P. and Garner, S. (2012). Acne vulgaris. *Lancet* **379**, 361-372.
Yagyu, H., Kitamine, T., Osuga, J.-i., Tozawa, R.-i., Chen, Z., Kaji, Y., Oka, T., Perrey, S., Tamura, Y., Ohashi, K. et al. (2000). Absence of ACAT-1 attenuates atherosclerosis but causes dry eye and cutaneous xanthomatosis in mice with congenital hyperlipidemia. *J. Biol. Chem.* **275**, 21324-21330.
Zhang, S., Shui, G., Wang, G., Wang, C., Sun, S., Zouboulis, C. C., Xiao, R., Ye, J., Li, W. and Li, P. (2014). Cidea control of lipid storage and secretion in mouse and human sebaceous glands. *Mol. Cell. Biol.* **34**, 1827-1838.
Zheng, Y., Prouty, S. M., Harmon, A., Sundberg, J. P., Stenn, K. S. and Parimoo, S. (2001). Scd3–a novel gene of the stearoyl-CoA desaturase family with restricted expression in skin. *Genomics* **71**, 182-191.